Short communication

# Morphology and electrical properties of carbon coated LiFePO$_4$ cathode materials

Bing Zhao[a], Yong Jiang[a], Haijiao Zhang[a,*], Haihua Tao[b], Mingyang Zhong[b], Zheng Jiao[b,**]

[a] Institute of Nanochemistry and Nanobiology, Shanghai University, Shanghai 200444, PR China
[b] School of Environmental and Chemical Engineering, Shanghai University, Shanghai 200444, PR China

## ARTICLE INFO

## ABSTRACT

Core-shell LiFePO$_4$@C composites were synthesized successfully from FePO$_4$/C precursor using the polyvinyl alcohol (PVA) as the reducing agent, followed by a chemical vapor deposition (CVD) assisted solid-state reaction in the presence of Li$_2$CO$_3$. Some physical and chemical properties of the products were characterized by X-ray powder diffraction (XRD), Raman, SEM, TEM techniques. The effect of morphology and electrochemical properties of the composites were thoroughly investigated. XRD patterns showed that LiFePO$_4$ has an order olivine structure with space group of *Pnma*. TEM micrographs exhibited that the LiFePO$_4$ particles encapsulated with 3-nm thick carbon shells. The powders were homogeneous with grain size of about 0.8 μm. Compared with those synthesized by traditional organic carbon source mixed method, LiFePO$_4$@C composite synthesized by CVD method exhibited better discharge capacity at initial 155.4 and 135.8 mAh g$^{-1}$ at 0.1C and 1C rate, respectively. It is revealed that the carbon layer coated on the surface of LiFePO$_4$ and the amorphous carbon wrapping and connecting the particles enhanced the electronic conductivity and rate performances of the cathode materials.

© 2008 Elsevier B.V. All rights reserved.

## 1. Introduction

There is an increasing demand for batteries with a high energy density for use in electric vehicle (EV) and hybrid electric vehicle (HEV). LiCoO$_2$ is used as the cathode material for commercial lithium batteries [1], but it falls short in meeting energy storage demands required by automotive industry in terms of high cost, thermal instability and environmental pollution. At present, LiFePO$_4$ is considered to be a promising candidate due to its ability to provide long cycle life and high rate [2]. Especially, the material has many excellent properties such as inexpensive, non-toxic and thermally stable in the fully charged state. More importantly, LiFePO$_4$ has a large theoretical capacity of 170 mAh g$^{-1}$ and good cycle stability [3]. Owing to its important behaviors and promising applications, the preparation and characterization of LiFePO$_4$ have attracted researcher's interests [4]. However, the poor rate capacity of LiFePO$_4$ seriously hinder and/or delay its further commercialization as a cathode material for Li-ion battery, because the separation of the chain of FeO$_6$ edge-shared octahedral contributes an extremely low electronic conductivity [5].

Hence, it is also a great challenge to find new synthesis methods for preparing LiFePO$_4$ in an effective way. Many efforts have been tried in the synthesis of LiFePO$_4$ in the attempt to improve

its rate capability by decreasing the size of the particles or forming carbon coatings around individual active particles [6,7]. Many researches have reported that LiFePO$_4$/C composites containing carbon or carbon coated LiFePO$_4$ could improve the electric conductivity of LiFePO$_4$ and exhibit excellent cathode performances [8–10]. However, the behavior of LiFePO$_4$/C composites depends on the phase purity of the active material, particle size, structure of the carbon additive and the carbon content [11]. The conventional synthesis route, in which the carbon source materials are simply mixed together with LiFePO$_4$ precursor, yields a non-uniform distribution of carbon in the final LiFePO$_4$/C composite.

In this work, we report a novel chemical vapor deposition (CVD) assisted solid-state route to synthesize carbon-coated LiFePO$_4$ cathode with polyvinyl alcohol (PVA) and benzene vapor as the reducing agent and carbon source. Core-shell LiFePO$_4$@C nanostructured composites were prepared via the CVD procedure. The electrochemical Li-ion intercalation performance of this material was tested and compared with that of LiFePO$_4$/C composite without CVD procedure.

## 2. Experimental

The starting materials were iron (III) phosphate (FePO$_4$·4H$_2$O) and lithium carbonate (Li$_2$CO$_3$). Firstly, the FePO$_4$·4H$_2$O and a certain amount of polyvinyl alcohol (29 g PVA per mole FePO$_4$) were mixed and pre-sintered at 600 °C under an inert atmosphere. During this procedure, the PVA was decomposed into amorphous carbon which then performed as the reducing agent of ferric phosphate. The black precursor and stoichiometric molar Li$_2$CO$_3$

* Corresponding author. Tel.: +86 21 6613 5276; fax: +86 21 6613 5275.
** Corresponding author. Tel.: +86 21 6998 2487; fax: +86 21 6998 2744.
E-mail addresses: hjzhang128@shu.edu.cn (H. Zhang), zjiao@shu.edu.cn (Z. Jiao).

were ball-milled in a stainless steel vessel for 3 h with a rotation speed of 100 rpm. The blend was then heated at 700 °C for 10 h to form LiFePO$_4$/C composite in a protecting atmosphere. The nitrogen and benzene vapor gas mixture were used to perform the chemical vapor deposition process, in which the N$_2$ was flowed into the benzene solution and measured by mass flowmeter.

During this process, the benzene vapor was adsorbed around the surface of the LiFePO$_4$ and carbonized at high temperature, forming carbon coating layer on the surface of LiFePO$_4$. For comparison, LiFePO$_4$/C composite sintered at 700 °C for 10 h in nitrogen was also prepared without CVD procedure.

X-ray powder diffraction (XRD) patterns were obtained on the Germany Bruker D8 Advance instrument operating at 40 kV and 40 mA using Cu Kα radiation (λ = 0.154 nm), scanning range 2θ from 15° to 70° with a step size of 0.02° and a constant counting time of 3 s per step. The powder morphology was observed by JEOL JSM-6700F (FESEM). The structural properties and the morphology of carbon were studied by a JSM-2010F high-resolution transmission electron microscopy (HRTEM). The Raman spectra were recorded on an Invia Raman Microscope System (Renishaw Co., Eng). For electrochemical measurements, the mixture of carbon-coated LiFePO$_4$ powder, carbon black, and polytetrafluoroethylene (PTFE) with a weight ratio of 85:10:5 was used as the cathode. An electrochemical 2016 coin cell consisted of the cathode, lithium foil as the anode and 1 M LiPF$_6$ in dimethyl carbonate (DMC), diethyl carbonate (DEC) and ethylene carbonate (EC) (1:1:1 by weight) as an electrolyte, and the celgard 2400 as the separator. The cells were galvanostatically charged and discharged between 2.5 and 4.2 V at ambient temperature. A constant current was set to a value between 10 and 500 mA g$^{-1}$ (corresponding roughly to C/10 and 5C, respectively).

## 3. Results and discussion

Recent studies [9,11–13] have shown a clear correlation between organic additive structure and cell capacity. Doeff and co-workers
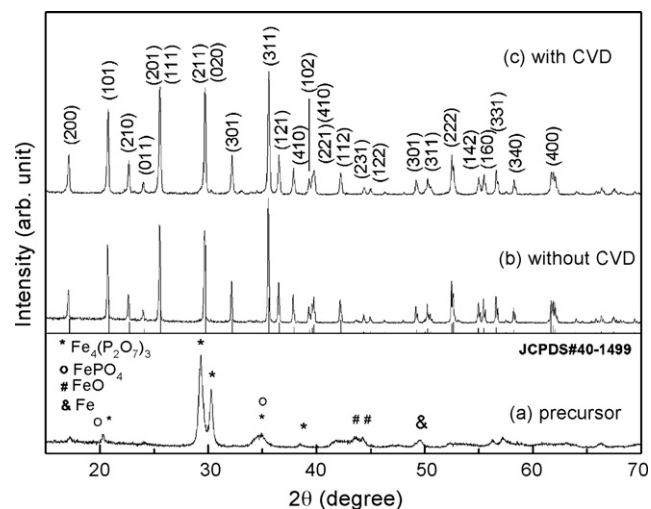


**Fig. 1.** XRD patterns of FePO$_4$ precursor (a) crystal LiFePO$_4$, (b) without CVD, (c) with CVD.

[9] have proposed several criteria to choose optimized organic compounds (i) undergoing decomposition rather than evaporation during the firing process, (ii) soluble in a common solvent for evenly distributed particle surfaces during sintering, and (iii) suitable functionalities for cyclic compound formation or compounds having aromatic or polyaromatic groups. Based on the above criteria, the benzene was selected as the carbon source and reducing agent. Meanwhile, it was considered that the aromatic hydrocarbon derivatives (toluene, naphthalene, biphenyl, etc.) could also be carbonized and form carbon coating on the surface of LiFePO$_4$.

Fig. 1 showed the XRD patterns of FePO$_4$ precursor and the crystallized LiFePO$_4$ synthesized at 700 °C for 10 h. We found that the FePO$_4$·4H$_2$O had been dehydrated and reduced partly during the



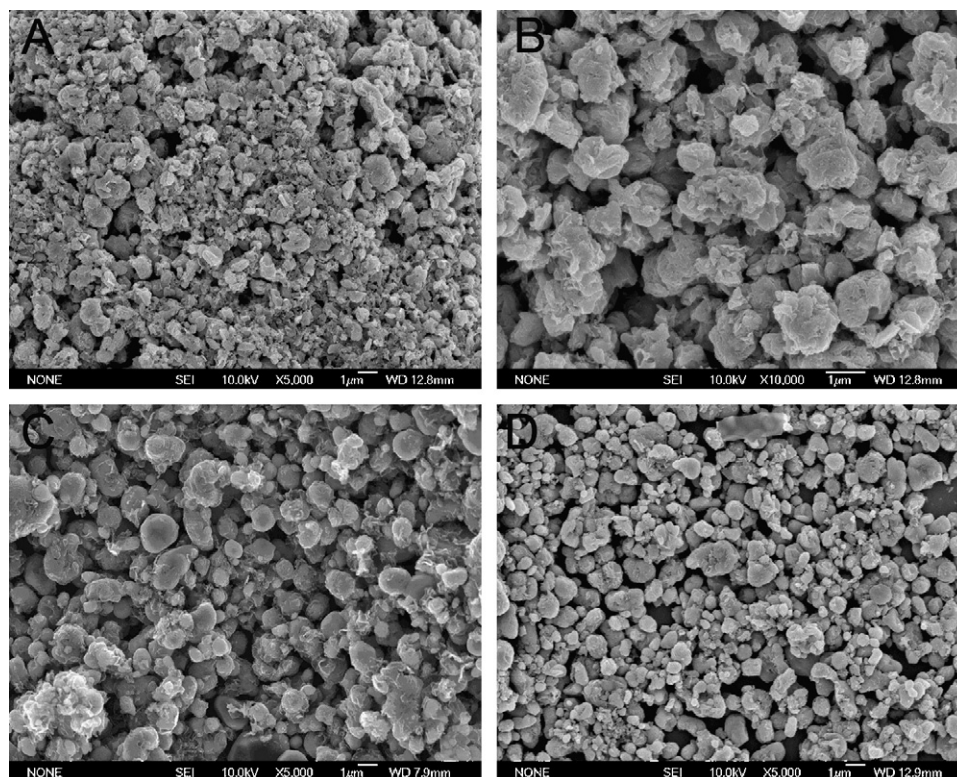**Fig. 2.** SEM micrographs of FePO$_4$ precursor (A ×5000; B ×10,000) and crystal LiFePO$_4$, (C) without CVD, (D) with CVD.

first calcination procedure. Apparently, the decomposition of PVA promoted the reduction and polycondensation of $FePO_4$ at high temperature. The diffraction peaks of $Fe_4(P_2O_7)_3$, FeO and even Fe could be found in the XRD pattern (Fig. 1(a)). Potassium dichromate titration testing showed that about 50–65% ferric content was reduced in divalent iron during this procedure. After sintering at 700 °C for 10 h, the precursor mixed with $Li_2CO_3$ could be synthesized to the pure $LiFePO_4$ phase whether with CVD procedure or not, as shown in Fig. 1(b) and (c). There was no evidence of diffraction peaks for carbon, possibly due to its amorphous structure. The amount of carbon in the composite without CVD procedure was about 9.7 wt% determined by the method introduced in other literature [14], but for the composite with CVD procedure, the carbon content had increased to 10.9 wt%. Although CVD method increased the carbon content just as low as about 1.2 wt%, the grain size indicated the growth of $LiFePO_4$ grains was effectively prevented by the formed carbons during the CVD process.

Fig. 2 was the SEM micrographs of $FePO_4$/C precursor (Fig. 2A and B) and crystallized $LiFePO_4$/C composites (Fig. 2C and D). The $FePO_4$/C precursor was amorphous and the carbon dispersed around the particles. From the high magnification micrograph ($\times$10,000, Fig. 2B), it was found that the compounds exhibited amorphous structure, which supplied a big specific surface area for the subsequent reactions. The final samples showed a globular structure with a grain size of about 1.2 and 0.8 μm, respectively. The product with CVD procedure exhibited a narrow grain size distribution and small particles, which was agreed with the result of the XRD patterns.

Normally using $FePO_4$ as the iron sources to synthesize $LiFePO_4$/C composite, a high carbon content was necessary to reduce trivalent iron to bivalent iron and get sufficient electric conductivity. It was also found that the carbon distribution and carbon morphology greatly influenced the electrochemical performance of the $LiFePO_4$/C composite [9,15,16]. Seen from the Fig. 3, there was a large amount of amorphous carbon wrapping and connecting the $LiFePO_4$ particles in the sample synthesized in pure nitrogen without CVD procedure, and no distinct carbon layer was observed on the surface of $LiFePO_4$ grains (Fig. 3B). However, besides nanometer-sized carbon webs wrapping and connecting the $LiFePO_4$ particles (as the arrow indicated in Fig. 3C), there were thin graphite shells encapsulating the $LiFePO_4$ particle in the samples synthesized in the mixed gas of nitrogen and benzene vapor with CVD procedure, just similar to the structure of carbon-coated $Li_3V_2(PO_4)_3$ and $LiFePO_4$ reported by other literatures [17,18]. It could be seen that the thickness of the graphite shell was about 3–5 nm (Fig. 3D). The thickness of the carbon shell could be controlled by varying the concentration of benzene vapor in protecting gas or the time of CVD process. There was no agglomeration after sintering, implying that the grain growth was restrained by the thin layer of the carbon on the surface of the grain.

During high temperature heating procedure, active hydrogen and gaseous hydrocarbons were generated from the pyrolysis of aromatic hydrocarbon, which provided a strong reductive atmosphere to reduce $Fe^{3+}$ to $Fe^{2+}$, consequently formation of $LiFePO_4$ crystal. The residual carbon coated on the surface of $LiFePO_4$ particles (Fig. 3C). From the Raman spectra of carbon films obtained by
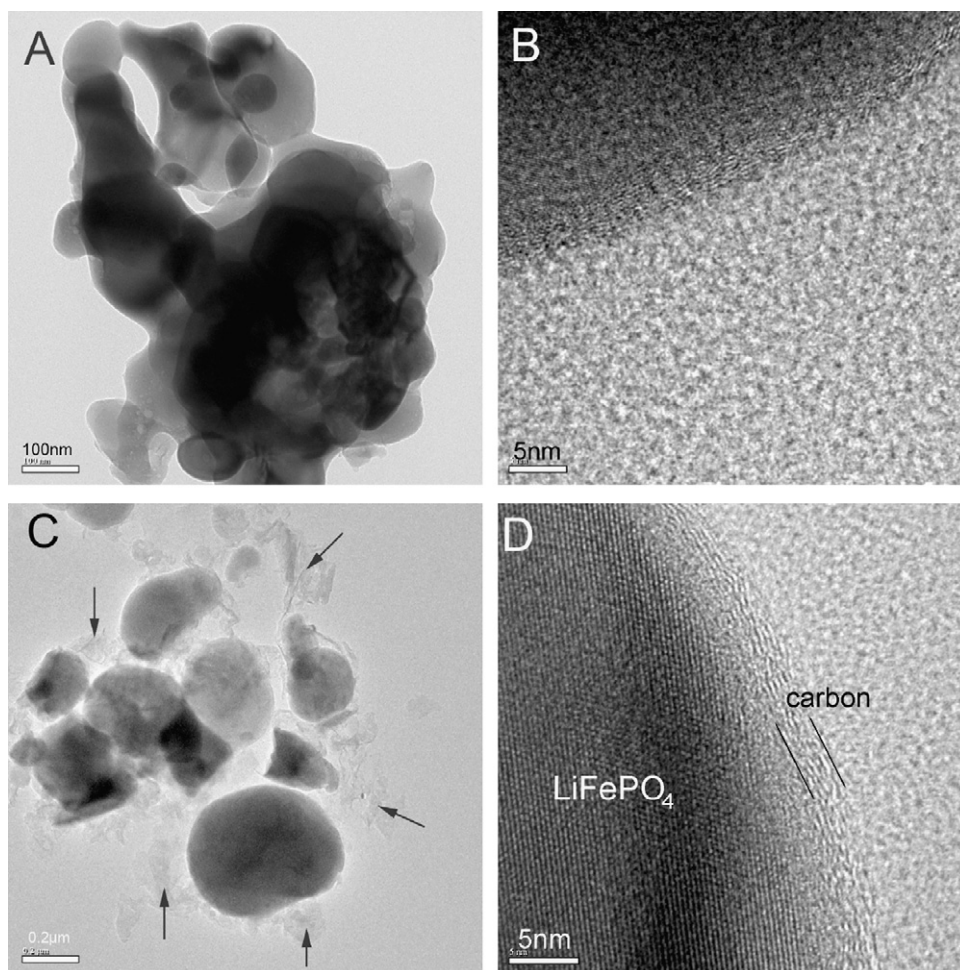


**Fig. 3.** TEM micrographs of $LiFePO_4$/C composites (A and B) without CVD, (C and D) with CVD.
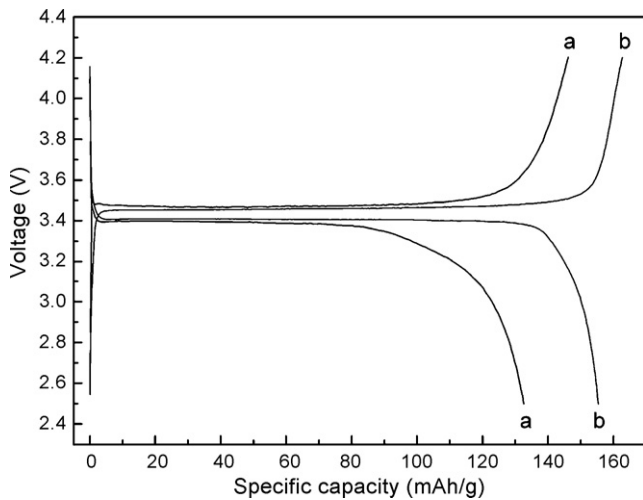
**Fig. 4.** Initial voltage profiles of LiFePO$_4$/C composites (a) without CVD, (b) with CVD.



**Fig. 6.** Rate (a) and cycle performances (b) of LiFePO$_4$/C composites.

pyrolysis of benzene (not shown here), the $I_D/I_G$ value was about 0.75–0.77, which of that without CVD was about 0.87. The former is much lower than the value in Ref. [9,19]. The low $I_D/I_G$ ratios indicated that the carbon film obtained by pyrolysis of benzene was highly graphitized carbons, which could also be identified from the 0.34 nm graphite layer distance in Fig. 3D. This highly graphitized carbon layer may help the core-shell LiFePO$_4$@C composites exhibit better electronic conductivity and lithium ion diffusibility.

Fig. 4 showed typical charge-discharge voltage profiles of LiFePO$_4$/C composites (a) without CVD and (b) with CVD. The tests were performed galvanostatically at a charge-discharge rate of C/10 in the range 2.5–4.2 V versus Li$^+$/Li. The charge–discharge profiles appeared with the typical voltage plateau (at 3.45 V vs Li$^+$/Li) attributed to the two-phase reaction of the $(1-x)$FePO$_4 + x$LiFePO$_4$ system. The LiFePO4@C composite with CVD procedure exhibited a reversible capacity of 155.4 mAh g$^{-1}$, corresponding to a utilization efficiency of 91.4%. But for the sample without CVD procedure, the plateau was little lower and shorter. The reversible capacity was about 132.6 mAh g$^{-1}$ with a severe polarization. This suggested that the shielded graphite layer and homogeneous carbon webs allowed a higher kinetic coefficient than the uneven amorphous carbon. This result was also confirmed by the cyclic voltammogram curves of two LiFePO$_4$/C composites shown in Fig. 5. The LiFePO$_4$@C composite behaved higher current peak intensity, smaller poten-
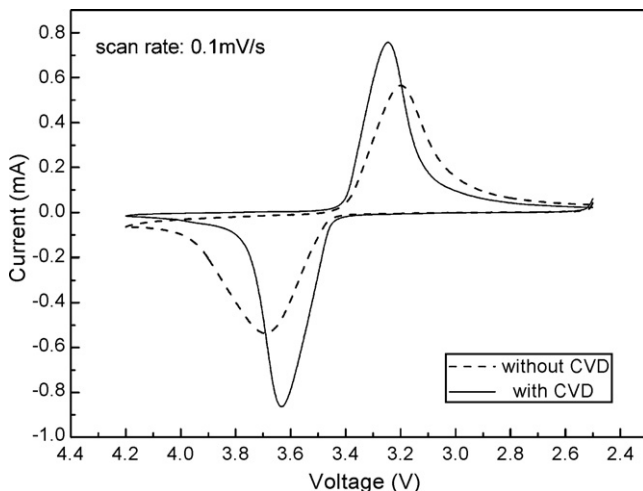
tial differences between anodic peak and cathodic peak and larger discharge capacity (curve area) than the one prepared without CVD.

The charge and discharge tests at various current rates ranging from 0.1 to 5C (1C = 170 mA g$^{-1}$) were performed and the results were shown in Fig. 6. For sample without CVD procedure, the discharge capacity was 132.6 mAh g$^{-1}$ (78.0% of theoretical capacity) at 0.1C. It decreased steeply to 66.5 mAh g$^{-1}$ (50.2% of its initial value) at the high current rate of 5C. To some extent, this was attributed to low diffusion rate of lithium ions for limiting the supply of electrons into the cathode materials [8,20]. But for sample with CVD procedure, the discharge capacity was 155.4 mAh g$^{-1}$ at 0.1C (91.4% of theoretical capacity) and 114.6 mAh g$^{-1}$ (73.7% of its initial value) at 5C, respectively. For Impedance spectroscopy, the electrical conductivity values of the materials with CVD and without CVD were $2.4 \times 10^{-2}$ and $6.7 \times 10^{-4}$ S cm$^{-1}$, respectively.

Long-term cyclic charge/discharge performances of the samples were shown in Fig. 6b. The discharge capacity of LiFePO$_4$@C is 136.8 mAh g$^{-1}$ after 30 cycles at 0.1C rate, much higher than LiFePO$_4$ without CVD procedure (108.6 mAh g$^{-1}$ after 30 cycles). The retention rate in discharge capacities was 91.8% for LiFePO$_4$@C composites but only 85.7% for LiFePO$_4$ without CVD procedure after 30 cycles. The constituents of the surface passive film (polycarbonates, polymeric hydrocarbons, Li$_2$CO$_3$, LiF, Li$_x$PF$_y$ and Li$_x$PF$_y$O$_z$) formed on the cathode particles during the electrochemical reaction changes with the oxide and electrolyte that increases the



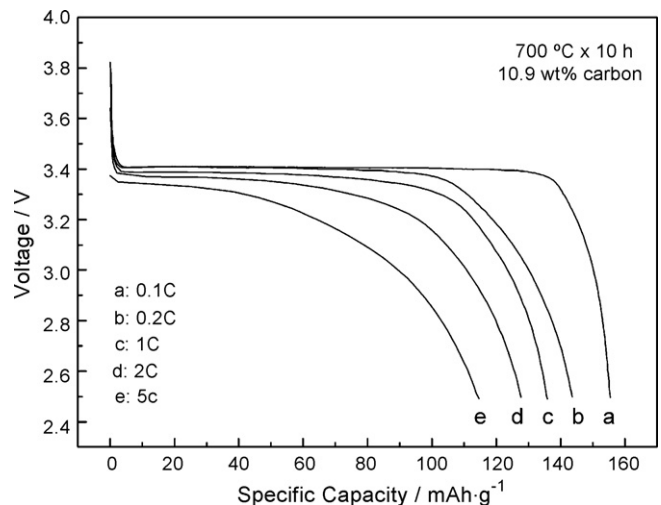**Fig. 5.** Cyclic voltammogram of LiFePO$_4$/C composites.



**Fig. 7.** Discharge curves of core-shell LiFePO$_4$@C composite prepared with CVD procedure at different discharge rates.

resistance of the surface film and dynamically hinders the movement of the lithium ion during the (de)lithiation process [21]. Thus, during cycling, the formation of a passive surface film, resulting in impedance growth of the $LiFePO_4/C$ resulted in faster capacity fade and lower cycle stability during repeated cycling compared to $LiFePO_4@C$ samples.

The discharge profiles of $LiFePO_4@C$ composites at different rates were shown in Fig. 7. All samples were charged at the same specific current of $34\,mA\,g^{-1}$ (0.2C rate) to insure identical initial conditions for each discharge. The electrode was able to deliver a specific capacity of $135.8\,mAh\,g^{-1}$ at 1 C rate, with a voltage plateau at about 3.35 V versus $Li^+/Li$. The capacities reached $127.7\,mAh\,g^{-1}$ at 2C rate and $114.6\,mAh\,g^{-1}$ at 5C rate, respectively. The high-rate discharge performance indicated that the synthesized $LiFePO_4@C$ composite would be well suited for cathode materials of high-power lithium batteries.

## 4. Conclusions

Core-shell $LiFePO_4@C$ composites were synthesized successfully via a chemical vapor deposition assisted solid-state reaction. TEM micrographs showed the $LiFePO_4$ particles encapsulated with thin graphite shell of 3 nm in thickness. The discharge capacity of $LiFePO_4@C$ was 155.4 and $135.8\,mAh\,g^{-1}$ at 0.1C and 1C rate, respectively. Furthermore, the capacity retention was 91.8% even after 30 cycles at a constant current density of $17\,mA\,g^{-1}$ (ca. 0.1C rate), much higher than that of the $LiFePO_4$ composite without graphite shell. With at higher discharge rate of 5C rate, the core-shell $LiFePO_4@C$ composites could keep a high specific capacity of $114.6\,mAh\,g^{-1}$. The above results indicated that the carbon layer coated on the surface of $LiFePO_4$ composite and the amorphous carbon wrapping and connecting the particles prevented the agglomeration of the $LiFePO_4$ and improved the conductivity of this material. The surface coverage of active materials would reduce the degradation of liquid electrolytes by suppressing the direct contact between them, which would contribute to the improvement of the cycle performance of the $LiFePO_4@C$ composites. In conclusion, the $LiFePO_4$ synthesized by our method showed high potential for cathode material for high-power lithium ion batteries.

## References

[1] K. Mizushima, P.C. Jones, P.C. Wiseman, J.B. Goodenough, Mater. Res. Bull. 15 (1980) 783–789.
[2] A.K. Padhi, K.S. Najundaswamy, J.B. Goodenough, J. Electrochem. Soc. 144 (1997) 1188–1194.
[3] S.H. Ju, Y.C. Kang, Mater. Chem. Phys. 107 (2008) 328–333.
[4] M.S. Whittingham, Y. Song, S. Lutta, P.Y. Zavalij, N.A. Chernova, J. Mater. Chem. 15 (2005) 3362–3379.
[5] S. Okada, S. Sawa, M. Egashira, J. Yamaki, M. Tabuchi, H. Kageyama, T. Konishi, A. Yoshino, J. Power Sources 97–98 (2001) 430–432.
[6] K. Zaghib, A. Mauger, F. Gendron, C.M. Julien, Chem. Mater. 20 (2008) 462–469.
[7] B. Boonchom, C. Danvirutai, Ind. Eng. Chem. Res. 46 (2007) 9071–9076.
[8] H.C. Kanga, D.K. Jun, B. Jin, E.M. Jin, K.H. Park, H.B. Gu, K.W. Kim, J. Power Sources 179 (2008) 340–346.
[9] J.D. Wilcox, M.M. Doeff, M. Marcinek, R. Kostecki, J. Power Sources 154 (2007) A389–A395.
[10] F. Sauvage, L. Laffont, J.M. Tarascon, E. Baudrin, J. Power Sources 175 (2008) 495–501.
[11] C.W. Ong, Y.K. Lin, J.S. Chen, J. Electrochem. Soc. 154 (2007) A527–A533.
[12] G.T.-K. Fey, T.L. Lu, J. Power Sources 178 (2008) 807–814.
[13] R.L. Wang, L.M. Moshurchak, J. Electrochem. Soc. 155 (2008) A66–A73.
[14] P.P. Prosini, D. Zane, M. Pasquali, Electrochim. Acta 46 (2001) 3517–3523.
[15] R. Dominko, M. Gaberscek, J. Drofenik, M. Bele, S. Pejovnik, J. Jamnnik, J. Power Sources 119–121 (2003) 770–773.
[16] Y.Q. Wang, J.L. Wang, J. Yang, J. Nuli, Adv. Funct. Mater. 16 (2006) 2135–2140.
[17] M.M. Ren, Z. Zhou, X.P. Gao, W.X. Peng, J.P. Wei, J. Phys. Chem. C 112 (2008) 5689–5693.
[18] R. Dominko, M. Bele, M. Gaberscek, M. Remskar, D. Hanzel, S. Pejovni, J. Jamnnik, J. Electrochem. Soc. 152 (2005) A607–A610.
[19] M.M. Doeff, Y. Hu, F. McLarnon, R. Kostecki, Electrochem. Solid-State Lett. 6 (2003) A207–A209.
[20] D.-Y.W. Yu, K. Donoue, T. Inoue, M. Fujimoto, S. Fujitani, J. Electrochem. Soc. 153 (2006) A835–A839.
[21] C.Z. Lu, J.M. Chen, Y.D. Cho, W.H. Hsu, P. Muralidharan, G.T.-K. Fey, J. Power Sources 184 (2008) A392–A401.